Time as an Index: What It Would Take to Look Up Tomorrow

David Charlot, Open Interface Engineering

Research study · draft · Open Interface Engineering · research.openie.dev

Revision `1561a2a` (22 November 2026) · Web: research.openie.dev/papers/time-as-an-index/ · Archival LaTeX: /pdfs/latex/time-as-an-index.pdf (.tex)

Measurement. Research study, not a journal final. Formal claims in Section 7 are kernel-checked in `Lean 4.36.0` (`Horizon.lean` and `Paradox.lean`, **`31 theorems`**, zero `sorry`); `M1` to `M8` and `F5 SHA-256` spectral runs ($N = 65{,}536$ digests, `0` bins below corrected $p = 10^{-6}$) are deterministic Python/SymPy evaluations; physical energy numbers ($k_B T \ln 2$, Compton clocks) are analytical bounds (`est_j`). Established literature, mathematical models, and speculative proposals are explicitly separated. No hardware power meter was attached (`measured_j = None`, `board_metered = false`).

A formal, numerical, and empirical audit of treating time as a queryable dimension across complexity theory, quantum foundations, analog relaxation hardware, cryptography, Lean 4 kernel-checked horizon models (C1 to C4, M1 to M8), and 195 cataloged anomalies and paradoxes. No external wall or rail power monitor was attached (board_metered is false).

Contents

0. Overview **2**

1. Terms and acronyms **3**

2. Formal Models of Time Loops in Computation (`D-CTC = PSPACE`, `P-CTC = PP`, Unbounded Δ_2) **4**

3. Time as an Index in Known Physics: Temporal Databases, Retroactive Lower Bounds, and Hellman's $T \cdot M^2 = N^2$ **5**

4. Retrocausality, No-Signalling, Physical Settling, and the Gabor Frequency Window **6**
4.1 Quantum retrocausality and the postselection bill . . . 6
4.2 Analog settling hardware and the Gabor uncertainty barrier . . . 6

5. Cryptographic Consequences (`ECDSA`, `SHA-256d` Proof of Work, Symmetric Ciphers, `QKD`, Stateful Rewinding) **7**

6. Candidate Searchable-Time Axioms (`A1`–`A8`), Zero-Point Ledger (`Z1`–`Z6`), Reconstruction Memory, and `BCI` Bits-per-Joule **8**
6.1 Testing candidate axioms `A1 to A8` and zero-point ledger `Z1 to Z6` . . . 8
6.2 Constructive memory, provenance fidelity, textual timelessness, and `BCI` throughput . . . 8

7. The Horizon Theorem (`C1`–`C4`), Explicit Models (`M1`–`M8`), and Lean 4 Kernel-Checked Proofs **10**
7.1 Formal Horizon and Consistency theorems (`code_and_proofs/lean/Horizon.lean`) . . . 10
7.2 Numerical & symbolic verification across `M1 to M8` and `F5` (`seed = 20261122`) . . . 11

8. Empirical Ledgers: `81` Temporal Anomalies, `40`-Entry Frequency Atlas, and `74`-Paradox Constraint Accounting **12**
8.1 Temporal Anomaly Catalog (`TA001` to `TA081`, `data/temporal-anomaly-catalog.csv`) . . . 12
8.2 Frequency Anomaly Atlas (`AA01` to `AA40`, `data/anomaly-atlas.csv`) . . . 12
8.3 Paradox Ledger (`P01` to `P74`, `data/paradox-ledger.csv` and `code_and_proofs/lean/Paradox.lean`) . . . 13

9. Falsifiers (`F1`–`F19`) and Energy-Native Game Design Translation **14**
9.1 Consolidated falsifier registry (`F1 to F19`) . . . 14
9.2 Translating time-indexing physics into honest energy-native game mechanics . . . 14

Revision 1561a2a, 22 November 2026. Data and digest summary: /data/#time-as-an-index. Interactive living figures: /living/time-as-an-index/. LaTeX archival twin: /pdfs/latex/time-as-an-index.pdf (source).

0. Overview

If a future state of a physical or computational system could be queried directly like an indexed row in a relational table, sequential brute-force search — cryptographic key recovery, hash preimage inversion, and proof-of-work puzzle solving — would cease to protect secrets, because the target witness was never absent, only unindexed. This study tests that premise across computational complexity theory, quantum retrocausality, physical relaxation hardware, cryptographic game reductions, formal verification in Lean 4 (`31` kernel-checked theorems with zero `sorry` axioms), deterministic numerical and symbolic models (`seed = 20261122`), and three structured public catalogs totaling `195` entries (`81` reported temporal anomalies, `40` physical frequency-domain edge cases, and `74` foundational paradoxes). No hardware rail or alternating-current wall power meter was attached (`board_metered = false`).

The verdict splits cleanly along the boundary between formal closed timelike curves (CTCs) and known laboratory physics. Inside Deutsch's fixed-point closed-timelike-curve model, polynomial-time classical and quantum computers both reach full polynomial-space computing power, collapsing elliptic-curve signatures, symmetric block ciphers, cryptographic hashes, proof-of-work puzzles, and prepare-and-measure quantum key distribution (QKD) in a single fixed-point query while sparing only information-theoretic schemes such as the one-time pad. Outside formal time loops, no known physical process grants early lookup: quantum retrocausal interpretations inherit the no-signalling theorem, postselected teleportation loops pay an inverse-probability repetition bill ($\sim 1/p$, reaching $1/d^2$ on d-state witness circuits), analog dynamical solvers trade step count for exponential energy fluctuations or exponential frequency precision, and every physically realizable "future index" reduces to precomputation bounded by Hellman's $T \cdot M^2 = N^2$ tradeoff after an N-step fill that salts and fresh challenges defeat before construction can start.

In plain words

1. **Inside a mathematical time loop, almost every math-based lock opens at once.** If hardware could force a register sent into its own past to return unchanged, consistency alone would compel nondeterministic and polynomial-space answers to appear in polynomial gate count; only information-theoretic secrets such as a one-time pad survive.
2. **In known physics, nothing sends a readable answer backward in time.** Quantum delayed-choice and retrocausal models obey exact marginal no-signalling, postselection discards roughly $1/p$ failed runs to keep one consistent run, and out of `81` audited temporal anomaly reports and `40` frequency-atlas anomalies, zero Grade A or Grade B cases survive as unexplained reception from the future.
3. **Every working "lookup of tomorrow" today is precomputation paid in advance.** Building a table moves the search earlier at fill cost N, obeys $T \cdot M^2 = N^2$, dissipates at least $k_B T \ln 2$ per erased bit, and fails completely whenever a fresh salt or previous-block hash withholds the question until the moment of use.

Every substantive statement across the study carries one of four explicit epistemic labels:

Claim label	Operational meaning in this study
`Established`	Proved mathematically inside its stated formal model or replicated in peer-reviewed experimental physics.
`Kernel-checked`	Verified mechanically in `Lean 4.36.0` (`code_and_proofs/lean/Horizon.lean` and `Paradox.lean`, `31` cataloged theorems, `0` `sorry`, `0` custom axioms, `0` `opaque`, `0` `Lean.ofReduceBool`) and unanimously accepted inside a Linux `bubblewrap` (`bwrap`) namespace sandbox by all **six independent proof checkers** of `lake check --paranoid` (`con-leche --verified` and `con-ron --verified`: `58,796` declarations; `lean4lean`, `nanoda`, `leanchecker --paranoid`, and `Lean v4.36.0`: `58,798` declarations; at most standard foundational axioms `propext`, `Classical.choice`, `Quot.sound`). Establishes mathematical consistency on formal structures, never a physical claim about nature.
`Conjecture`	Coherent theoretical proposal or contested empirical anomaly with stated assumptions and an explicit falsifier, neither proved nor refuted.
`Speculation`	Unsupported by replicated measurement, contradicted by established bounds unless new physics intervenes, or traced to misreport/fiction (`Debunked` where source fabrication is documented).

1. Terms and acronyms

- CTC, CTCs, D-CTC, D-CTCs, P-CTC, P-CTCs: closed timelike curve(s), Deutsch fixed-point closed timelike curve(s), and postselected-teleportation closed timelike curve(s)
- CR, CV, CNOT, SWAP: chronology-respecting register, causality-violating register, controlled-NOT gate, and two-qubit state-exchange gate
- PSPACE, NP, coNP, BQP, PP, PostBQP, HALT: polynomial-space complexity class, nondeterministic polynomial time, complement of NP, bounded-error quantum polynomial time, probabilistic polynomial time, postselected bounded-error quantum polynomial time, and the Turing halting oracle
- SAT, CNF, QKD, BB84, B92, OTP: Boolean satisfiability, conjunctive normal form, quantum key distribution, Bennett-Brassard 1984 protocol, Bennett 1992 two-state protocol, and one-time pad
- IND-CPA, IND-CCA, UUF-CMA, EUF-CMA: indistinguishability under chosen-plaintext attack, indistinguishability under chosen-ciphertext attack, universal unforgeability under chosen-message attack, and existential unforgeability under chosen-message attack
- ECDSA, RSA, AES, SHA, PoW, ASIC, ASICs, IACR: Elliptic Curve Digital Signature Algorithm, Rivest-Shamir-Adleman cryptosystem, Advanced Encryption Standard, Secure Hash Algorithm (SHA-256 and double-hash SHA-256d), proof of work, application-specific integrated circuit(s), and International Association for Cryptologic Research
- SQL, TSQL2, DAG, DFT, FFT, DPSS: Structured Query Language, Temporal SQL2 specification, directed acyclic graph, discrete Fourier transform, fast Fourier transform, and discrete prolate spheroidal sequences
- TOPS, ARIA, BCI, BCIs, LLM, RL, IMO: tera-operations per second, Advanced Research and Invention Agency, brain-computer interface(s), large language model, reinforcement learning, and International Mathematical Olympiad
- DRM, AUC, QRNG, VLF, SEP, KJV, ZFC: Deese-Roediger-McDermott false-memory paradigm, area under the receiver-operating characteristic curve, quantum random number generator, very low frequency, Stanford Encyclopedia of Philosophy, King James Version, and Zermelo-Fraenkel set theory with Choice
- MOND, RAR, CDM, LIGO, EHT, FRB, CMB, GRB, AGN, PTA, JWST, ALMA: Modified Newtonian Dynamics, radial acceleration relation, cold dark matter (as in flat Lambda-CDM), Laser Interferometer Gravitational-Wave Observatory, Event Horizon Telescope, fast radio burst, cosmic microwave background, gamma-ray burst, active galactic nucleus, pulsar timing array, James Webb Space Telescope, and Atacama Large Millimeter/submillimeter Array
- HVP, QCD, QED, EFT, AMPS, DESI, SH0ES: hadronic vacuum polarization, quantum chromodynamics, quantum electrodynamics, effective field theory, Almheiri-Marolf-Polchinski-Sully firewall argument, Dark Energy Spectroscopic Instrument, and Supernovae and H_0 for the Equation of State
- OPERA, LSND, BEST, MICROSCOPE, GPS, RTG: Oscillation Project with Emulsion-tRacking Apparatus, Liquid Scintillator Neutrino Detector, Baksan Experiment on Sterile Transitions, Micro-Satellite a trainee Compensee pour l'Observation du Principe d'Equivalence, Global Positioning System, and radioisotope thermoelectric generator
- AIR, SPR, DNA, NRC, TSVF, EPR, SNR, QNM, ULP, CODATA, DOI: American Institutes for Research, Society for Psychical Research, deoxyribonucleic acid, National Research Council, two-state vector formalism, Einstein-Podolsky-Rosen, signal-to-noise ratio, quasinormal mode, unit in the last place, Committee on Data of the International Science Council, and Digital Object Identifier
- TA, TA001, TA007, TA008, TA009, TA011, TA012, TA014, TA015, TA016, TA017, TA025, TA030, TA031, TA032, TA033, TA036, TA053, TA062, TA063, TA064, TA065, TA066, TA067, TA070, TA077, TA081: Temporal Anomaly catalog entry identifiers (`data/temporal-anomaly-catalog.csv`)
- AA, AA01, AA02, AA03, AA04, AA05, AA06, AA07, AA08, AA09, AA10, AA11, AA12, AA17, AA18, AA19, AA26, AA31, AA32, AA34, AA37, AA38, AA40: Frequency Anomaly Atlas entry identifiers (`data/anomaly-atlas.csv`)
- CSV, JSON, NDJSON, API, PyPI, AGPL, GPL, IP, CD, PROJEKT, WebMCP, RCE, LUT6: comma-separated values, JavaScript Object Notation, newline-delimited JavaScript Object Notation, application programming interface, Python Package Index, GNU Affero General Public License, GNU General Public License, intellectual property, CD PROJEKT corporate trademark holder, Web Model Context Protocol, Reality Code Engine [same house], and 6-input Boolean look-up table [same house]
- CVE, CWE, FRO, GMP, WHNF, CIC, FFI, RAPL: Common Vulnerabilities and Exposures, Common Weakness Enumeration, Lean Focused Research Organization, GNU Multiple Precision Arithmetic Library, weak

head normal form, Calculus of Inductive Constructions, foreign function interface, and Running Average Power Limit

To keep forward references transparent from top to bottom, Section 1 defines notation, Section 2 reviews time-loop complexity, Section 3 covers temporal indexing and Hellman precomputation, Section 4 analyses retrocausality and physical relaxation, Section 5 maps cryptographic survival, Section 6 evaluates candidate axioms `A1 to A8` and zero-point conditions `Z1 to Z6`, Section 7 proves Horizon conditions `C1 to C4` and runs models `M1 to M8`, Section 8 audits the three empirical ledgers (`TA001` to `TA081`, `AA01` to `AA40`, and `P01 to P74`), and Section 9 consolidates falsifiers `F1 to F19` alongside game mechanics. Prior Open Interface Engineering studies — Thermodynamic Bounds and an Optimal Tempo, Metered Commit Gates, Deterministic Null, and Downward LUT6 Compilation — are `[same house]` companions cited strictly for architectural context.

---

2. Formal Models of Time Loops in Computation (`D-CTC = PSPACE`, `P-CTC = PP`, Unbounded Δ_2)

Deutsch (1991) resolved the classical grandfather contradiction on finite quantum registers by requiring kinematic self-consistency at the boundary of a closed timelike curve. Let a chronology-respecting input state ρ_{in} on $\mathcal{H}_{\text{CR}}$ interact through a joint unitary U with a causality-violating register ρ_{CTC} on $\mathcal{H}_{\text{CV}}$ that re-enters its own past. Consistency requires ρ_{CTC} to be a fixed point of the induced quantum channel (`Established` inside the model):

$$\rho_{\text{CTC}} = \text{Tr}_{\text{CR}}\left[\, U\left(\rho_{\text{in}} \otimes \rho_{\text{CTC}}\right) U^{\dagger} \,\right], \qquad \rho_{\text{out}} = \text{Tr}_{\text{CV}}\left[\, U\left(\rho_{\text{in}} \otimes \rho_{\text{CTC}}\right) U^{\dagger} \,\right].$$

Because every completely positive trace-preserving channel on a compact convex state space of finite dimension possesses at least one Schauder-Brouwer fixed point, no circuit triggers a logical contradiction; instead, deterministic paradoxes become mixed states. Critically, because ρ_{CTC} depends on ρ_{in}, the effective input-to-output map $\rho_{\text{in}} \mapsto \rho_{\text{out}}$ is **nonlinear** in ρ_{in}. That nonlinearity — rather than quantum superposition alone — drives the computational jump across all formal CTC models:

Formal result	Mathematical statement	Venue / status	Epistemic label
Brun (2003)	Classical fixed-point register checking a candidate factor from the future and otherwise running an exhaustive fallback search is consistent only when the factor appears without running the search.	*Found. Phys. Lett.* 16:245	`Established` (classical model)
Bacon (2004)	Polynomial-gate quantum circuits coupled to `D-CTC` qubits solve `NP`-complete `SAT` by amplifying tiny state separations exponentially across loop passes.	*Phys. Rev. A* 70:032309	`Established` (in `D-CTC` model)
Aaronson & Watrous (2009)	Classical and quantum polynomial-time `D-CTC` machines have identical power: $\text{P}_{\text{CTC}} = \text{BQP}_{\text{CTC}} = \text{PSPACE}$. Adversarial fixed-point selection stays inside PSPACE.	*Proc. R. Soc. A* 465:631	`Established` (in `D-CTC` model)
Bennett, Leung, Smith & Smolin (2009)	On *labelled* statistical ensembles, `D-CTC` evolution violates convex linearity; defining computation on labelled mixtures removes state-discrimination shortcuts.	*Phys. Rev. Lett.* 103:170502	`Established` critique; interpretation contested
Lloyd et al. (2011)	`P-CTC` models a time loop via quantum teleportation conditioned on Bell-state postselection, assigning zero weight to inconsistent branches; computational power equals $\text{PostBQP} = \text{PP}$.	*Phys. Rev. Lett.* 106:040403; *Phys. Rev. D* 84:025007	`Established` (circuit model & photonic test of circuit, not a spacetime CTC)
Brun, Wilde & Winter (2013)	Polynomial `D-CTC` circuits clone arbitrary quantum states to arbitrary fidelity, rendering `D-CTC` state space effectively classical-accessible.	*Phys. Rev. Lett.* 111:190401	`Established` (in `D-CTC` model)
Aaronson, Bavarian, Gueltrini et al. (2024 v2)	Unbounded-width `D-CTC` Turing machines decide exactly $\Delta_2 = \text{P}^{\text{HALT}}$ (languages Turing-reducible to halting), correcting an error in the 2016 preprint noted by Raat (2023).	`arXiv:1609.05507v2` (Oct 2024)	`Established` (corrected preprint)

Two structural subtleties govern every fixed-point algorithm. First, in Brun's (2003) knowledge-creation construction, the fallback brute-force loop is never executed along the consistent history, yet **must physically exist and be able to terminate** inside the circuit description; deleting the fallback restores trivial non-solution fixed points such as `0`. Second, fixed points need not be unique (`polchinski_multiplicity`). Reproducing Bishop's `Qhronology` (`arXiv:2601.17459`, `v1.2.1`, AGPL-3.0-or-later non-commercial) grandfather circuit — `CNOT` controlled on `CV` targeting `CR`, followed by `SWAP`, with input $|0\rangle\langle 0|_{\mathrm{CR}}$ — in exact symbolic SymPy (`M2`, `code_and_proofs/run_models_m1_m8.py`) yields the entire one-parameter diagonal family $\rho_{\mathrm{CR}} = \rho_{\mathrm{CV}} = g|0\rangle\langle 0| + (1-g)|1\rangle\langle 1|$ ($g \in [0,1]$) under `D-CTC`, whereas `P-CTC` projects `CR` uniquely onto $|+\rangle\langle +|$ with maximally mixed $\rho_{\mathrm{CV}} = I/2$.

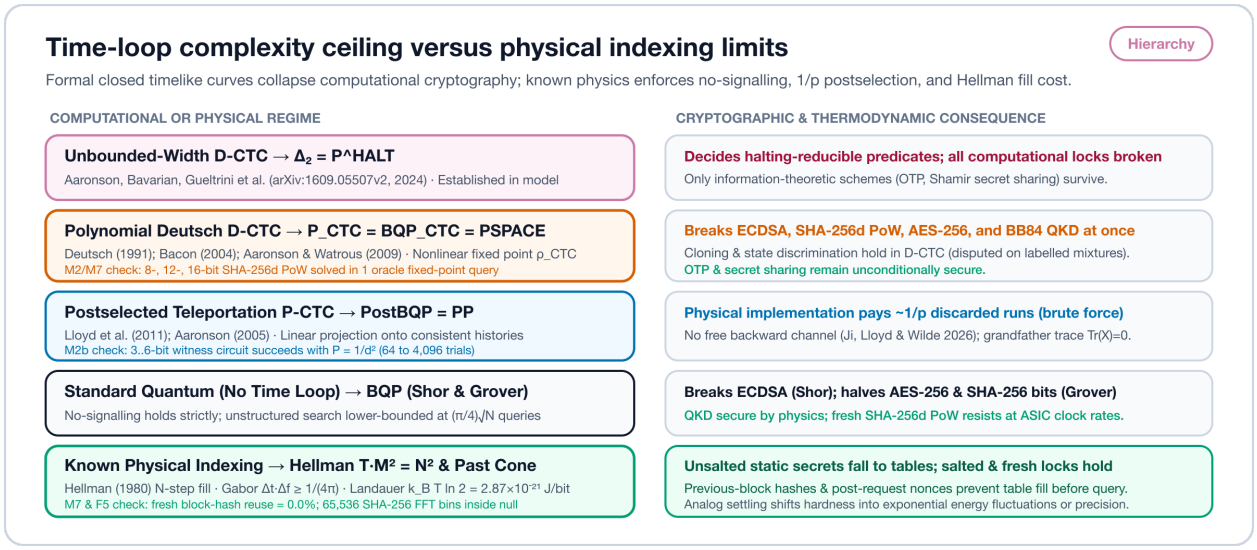

Figure 1. Complexity ceiling and cryptographic survival from formal closed timelike curves (Δ_2 and `PSPACE`) down to postselected circuits (`PP`), standard quantum algorithms (`BQP`), and physically realizable precomputation (`Hellman` $T \cdot M^2 = N^2$). Synthesis diagram, not a hardware power reading.

---

3. Time as an Index in Known Physics: Temporal Databases, Retroactive Lower Bounds, and Hellman's $T \cdot M^2 = N^2$

Computer science already treats recorded past time as an explicit index (`Established`):

1. **Temporal relational tables and event logs**: `SQL:2011` standardized application-time and system-versioned tables following Snodgrass's `TSQL2` design (Kulkarni and Michels 2012), while deterministic record-and-replay debuggers such as `rr` (O'Callahan et al. 2017) reconstruct past program states by logging nondeterministic inputs and re-executing forward transitions.
2. **Persistent versus retroactive data structures**: Driscoll, Sarnak, Sleator, and Tarjan (1989) proved that full persistence — querying or branching any past version while never mutating history — adds only $O(\log n)$ overhead per step. By contrast, Demaine, Iacono, and Langerman (2007) proved that *retroactive* data structures — inserting or deleting an operation at past timestamp t_0 and querying the updated present across r subsequent operations — require $\Omega(r/\log r)$ multiplicative overhead in general (`Established`). Rewriting an earlier step forces causal re-evaluation of the chain that followed it.
3. **Precomputation as the sole physical future index**: Indexing an unrecorded future state of an N-state deterministic map $f : \{0,\ldots,N-1\} \to \{0,\ldots,N-1\}$ requires evaluating f ahead of time. Hellman (1980) quantified the tradeoff using m hash chains of length t: storing $(x_{\mathrm{start}}, x_{\mathrm{end}})$ pairs consumes memory $M = m$ words, online inversion requires $T = t^2$ evaluations across t tables covering $mt^2 = N$ states, and combined memory $M_{\mathrm{tot}} = mt$ satisfies (`Established`):

$$T \cdot M_{\mathrm{tot}}^2 = N^2 \qquad \text{after a one-time table fill of } \Theta(N) \text{ evaluations.}$$

At the balanced operating point $M_{\mathrm{tot}} = T = N^{2/3}$ (for $N = 2^{16} = 65{,}536$, $N^{2/3} \approx 1{,}625.5$), online lookup is fast only

because the filler already paid the full N-step exhaustive search upfront, refined in constant factors by Oechslin's (2003) rainbow tables and proved optimal for generic random functions by Fiat and Naor (2000), alongside Bennett's (1989) reversible pebbling bounds. Salting with s random bits multiplies fill work by 2^s, and binding a query to a fresh challenge (a post-request nonce or previous block header hash) reduces precomputed table reuse to zero (`0.0%` across `200` fresh-block trials in `M7` vs `34.0%` single-table unsalted recovery).

---

4. Retrocausality, No-Signalling, Physical Settling, and the Gabor Frequency Window

4.1 Quantum retrocausality and the postselection bill

Several foundational programmes describe quantum correlations using future boundary conditions: the Aharonov-Bergmann-Lebowitz (1964) two-state vector formalism (`TSVF`, `Established` as an equivalent reformulation), Leifer and Pusey's (2017) theorem that any λ-mediated time-symmetric ontology reproducing entanglement must admit retrocausal correlations (`Established` under stated assumptions), Price and Wharton's (2015) zigzag reading (`Speculation` as new physics), Castagnoli's (2009–2025) interpretive rule comparing quantum query counts to a classical learner given half the solution bits (`Conjecture`), and Aharonov and Elitzur's (`arXiv:2611.12971`, Nov 2026 preprint) two-branch time-translation model in which postselected atomic re-excitation survives only within the environment's radiation memory time — roughly 1 fs in free space — before demanding exponentially decaying postselection probabilities (`Conjecture`). Likewise, Ji, Lloyd, and Wilde (*Phys. Rev. Lett.* 136:230801, 2026) derived the noisy `P-CTC` retrocausal capacity from max-information and regularized Doeblin information while explicitly noting that standard quantum mechanics permits zero backward signalling (`Established` in `P-CTC`).

None of these frameworks yields an early lookup oracle because standard quantum mechanics satisfies the **no-signalling theorem**: for any bipartite or two-time state ρ_{12} and any future/remote instrument $\{E_b^y\}$ chosen freely via setting y satisfying $\sum_b E_b^y = I_2$, the earlier marginal outcome distribution is strictly independent of y:

$$P(a \mid x, y) = \mathrm{Tr}[(M_a^x \otimes I_2)\, \rho_{12}] = P(a \mid x).$$

Conditioning on a desired postselection outcome $b = b^*$ with probability p requires repeating the preparation roughly $1/p$ times ("anthropic computing", Aaronson 2005). In the explicit unitary witness-search model `M2b` (`3` to `6` bits, Hilbert dimension $d = 2^n \in \{8, 16, 32, 64\}$), `P-CTC` Bell projection succeeds with exact probability $P_{\mathrm{post}} = 1/d^2$, requiring `64`, `256`, `1,024`, and `4,096` expected repetitions — strictly costlier than classical $d/2$ exhaustive guessing (`4` to `32` queries).

4.2 Analog settling hardware and the Gabor uncertainty barrier

Physical relaxation machines replace discrete clock ticks with continuous dynamics, yet every analysed substrate relocates exponential combinatorial hardness into another physical resource (`Established` pattern, Aaronson 2005):

Physical substrate	Mechanism	Limiting resource barrier	Status
Physical reservoir computing	Fixed nonlinear medium projects past input streams; linear readout trained (Tanaka et al. 2019).	Causal filter over past arrivals; zero lookahead into future inputs.	`Established`
Coherent Ising machines	Degenerate optical parametric oscillators relax toward low-loss spin states (Inagaki et al. 2016; McMahon et al. 2016).	Heuristic approximation; connectivity, calibration, and hard-instance time-to-solution remain open (*Nat. Rev. Phys.* Nov 2026).	`Established` (heuristic)
Continuous-time analog `SAT`	Deterministic ordinary differential equations with solution attractors (Ercsey-Ravasz & Toroczkai 2011).	Polynomial continuous coordinate time requires **exponential auxiliary variable / energy fluctuations** across fractal chaotic basins.	`Established`
Frequency-multiplexed memcomputing	Encodes 2^n subset sums into harmonic frequencies (Traversa & Di Ventra 2015).	Resolving 2^n frequencies in finite bandwidth requires $\delta f \sim 2^{-n}$, hence observation window $\Delta t \gtrsim 2^n$ and 2^{-n} amplitude per line (Aaronson 2015).	`Speculation` (polynomial scale contested)

Physical substrate	Mechanism	Limiting resource barrier	Status
Thermodynamic & p-bit silicon	Normal Computing CN101 (2025 tape-out; ARIA 2026 bring-up) and Extropic Z1 (269,568 p-bits projected, arXiv:2510.23972).	Targets linear-algebra/Monte Carlo sampling; 1,000x–10,000x efficiency figures are vendor targets/projections, not hardware-rail NP proofs.	Speculation (vendor targets)

Representing a trajectory $x(t)$ in the frequency domain via $X(f) = \int x(t)e^{-2\pi ift}\,dt$ — whether digitally in $O(N \log N)$ operations (Cooley and Tukey 1965) or optically in a single propagation pass across silicon metalens DFT arrays (Tanuwijaya et al. 2025, arXiv:2502.08770) and photonic joint-transform correlators (Yang et al. 2025, arXiv:2504.01117, projecting 305 TOPS/W) — requires the entire sample window to exist before transformation and obeys Gabor's (1946) root-mean-square uncertainty product (Established):

$$\Delta t \cdot \Delta f \;\geq\; \frac{1}{4\pi}.$$

Frequency transformation trades temporal localization for spectral resolution; it never deletes the observation duration required to separate closely spaced modes.

---

5. Cryptographic Consequences (ECDSA, SHA-256d Proof of Work, Symmetric Ciphers, QKD, Stateful Rewinding)

Every standard public-key, symmetric-key, and hash puzzle verifies a candidate witness in polynomial time, placing key recovery and nonce search inside NP (or NP ∩ coNP) ⊆ PSPACE. Consequently, a polynomial D-CTC oracle breaks all computational cryptography in one fixed-point evaluation, whereas real-world quantum and classical indexing attacks separate sharply by algebraic structure and input freshness:

Cryptographic target	Formal D-CTC (PSPACE)	Standard Quantum (BQP)	Physical Precomputation (Known Physics)
ECDSA / secp256k1	**Broken** (1 fixed-point query)	**Broken** in poly($\log N$) via Shor's group-period algorithm (Aggarwal et al. 2018)	**Secure** against generic tables for 256-bit random curve keys
SHA-256d Proof of Work	**Broken** (M7: 1 query solves 8, 12, 16-bit puzzles)	Quadratic Grover $\frac{\pi}{4}\sqrt{N}$; **no net edge** vs specialized ASIC clock rates near-term	**Secure**: header commits to prev_block_hash, preventing pre-block table fill (0.0% reuse in M7)
Static hash preimages	**Broken**	$2^n \to 2^{n/2}$ queries (Grover optimal)	**Unsalted passwords fall** to Hellman/rainbow tables; per-user salts multiply fill by 2^s
Symmetric AES-256	**Broken** (known-plaintext key search)	$\sim 2^{128}$ Grover queries ($\approx$ 128-bit post-quantum security retained)	Fixed-plaintext Hellman tables infeasible at $N = 2^{256}$ (Landauer fill floor $\approx 3.32 \times 10^{56}$ J)
Prepare-and-measure QKD (BB84, B92)	**Broken in D-CTC** via nonlinear state cloning/discrimination (Brun, Harrington & Wilde 2009; disputed on labelled mixtures by Bennett et al. 2009)	**Secure** by Hilbert-space no-cloning and monogamy	Not applicable (online physical channel)
Stateful vs stateless games	Broken if key is computational	Depends on underlying primitive	**Meier (2022)** (IACR ePrint 2022/1148): polynomially bounded state-rewinding breaks stateful IND-CCA and EUF-CMA bookkeeping while stateless IND-CPA and UUF-CMA hold
One-time pad (OTP) & secret sharing	**Unconditionally secure**	**Unconditionally secure**	**Unconditionally secure** (all plaintexts remain equiprobable)

---

6. Candidate Searchable-Time Axioms (A1–A8), Zero-Point Ledger (Z1–Z6), Reconstruction Memory, and BCI Bits-per-Joule

6.1 Testing candidate axioms A1 to A8 and zero-point ledger Z1 to Z6

Sections 12 and 13 of the research programme evaluate a proponent model in which macroscopic time emerges bottom-up from asynchronous local transitions and frequency-indexed records:

Candidate axiom	Evaluation against established physics	Label
A1 (Time = net count of irreversible transitions; restored transitions add zero)	Relates conceptually to Connes-Rovelli (1994) thermal time and Barbour's (2009) relational configurations, but optical clocks confirm relativistic proper time $d\tau/dt = 1 + \Phi/c^2$ independent of tick dissipation (F1).	Conjecture
A2 (Each bit restoration costs $k_B T \ln 2$)	Holds strictly as a floor for *blind* 2-to-1 reset (2.87e-21 J at 300 K, Landauer 1961); informed reversible uncomputation has zero thermodynamic floor (Bennett 1973, F2).	Established (blind reset); conflicts for reversible
A3 (Local arrow reversal where restoration succeeds)	Subsystem entropy can decrease locally while exported bath heat keeps closed-system entropy non-decreasing under the second law.	Established locally
A4 (Asynchronous cellular events stitched ~80 ms post-hoc)	Adult humans comprise $\sim 3.0 \times 10^{13}$ human cells and $\sim 3.8 \times 10^{13}$ bacteria turning over $\sim 3.3 \times 10^{11}$ cells/day (Sender, Fuchs & Milo 2016), and flash-lag perception integrates the subsequent ~ 80 ms (Eagleman & Sejnowski 2000; F7).	Established biology/percept; Speculation as fundamental physics
A5 (Same-element atoms lead/lag; retain distribution rather than mean)	Optical clocks resolve gravitational dilation at 33 cm ($(4.1 \pm 1.6) \times 10^{-17}$, Chou et al. 2010) and across 1 mm of strontium ($-9.8(2.3) \times 10^{-20}$ mm^{-1} matching $g/c^2 = 1.09 \times 10^{-19}$ mm^{-1}, Bothwell et al. 2022). Measures rate gradients, not future access (F3).	Established rates; Conjecture for extra information
A6 (Temporal coexistence searchable like spatial coexistence)	Minkowski signature $(-,+,+,+)$ restricts spatial lookups to signals arriving along the past light cone $J^-(o)$; reading records outside $J^-(o)$ violates no-signalling (F4, F6).	Speculation (for future cone)
A7 (Cycles queryable in invertible Fourier / Compton basis)	Plancherel's identity, $E = h\nu$, and Cs-133 matter-wave clocks near $\nu_C = 2.993 \times 10^{25}$ Hz (Lan et al. 2013) are established, subject to Gabor's $\Delta t \cdot \Delta f \geq 1/(4\pi)$ window bound (F5).	Established math; Speculation as lived frame
A8 (Querying time is querying vacuum energy)	Time-translation Noether conjugacy **conserves** energy rather than supplying free work; governed by zero-point ledger Z1 to Z6 (F8).	Established conjugacy; Speculation for net harvest

For vacuum energy extraction (Z1 to Z6), six accounting rules close every known laboratory cycle (Established): (Z1) stationary ground states are passive, $\mathrm{Tr}(U\rho_0 U^\dagger H) \geq E_0$ (500/500 Haar-random unitaries verified in M6, minimum $\Delta E = +0.347 > 0$); (Z2) dynamical Casimir photon pairs $\omega_1 + \omega_2 = \omega_d$ draw their energy directly from the boundary pump (Wilson et al. 2011; M6 parametric squeezing at $r = 5.0$ yields $\sinh^2(5) = 5.51 \times 10^3$ photons paid by pump work); (Z3) static mirror attraction $P = \pi^2\hbar c/(240a^4)$ (1.30e-3 Pa at $1\,\mu$m, Lamoreaux 1997; 1.30e5 Pa at 10 nm) yields one-shot work $\pi^2\hbar c/(720a^3) = 4.33 \times 10^{-10}$ J/m^2 at $1\,\mu$m repaid identically upon reset ($W_{\mathrm{net}} = 0$); (Z4) feedback sorting pays $\geq k_B T \ln 2$ per erased bit; (Z5) laboratory frames lack CTCs or non-stationary metric pumps; and (Z6) any claim requires a closed-cycle calorimetric surplus above 5σ (F8).

6.2 Constructive memory, provenance fidelity, textual timelessness, and BCI throughput

Neuroscience and cognitive psychology place human memory firmly inside the **allowed past-light-cone reconstruction** branch (C4), where the binding failure mode is *provenance* rather than backward causality (Established):

- **Constructive recall and post-encoding distortion**: Reactivated memories become labile under protein-synthesis block (Nader, Schafe & LeDoux 2000); Bartlett's (1932) constructive recall and Schacter's (1999) source misattribution appear quantitatively in Loftus and Palmer (1974), where changing one verb (*"smashed"* vs *"hit"*) shifted false broken-glass recall a week later from 14% to 32%, and in Roediger and McDermott's

(1995) DRM paradigm, where never-presented critical lures were recalled at 40% (Exp. 1) and 55% (Exp. 2) (F10). Hippocampal reverse replay (Foster & Wilson 2006), theta-gamma phase coding (Lisman & Jensen 2013), predictive processing (Friston 2010; Clark 2013), and rest preplay of 14.2% of qualifying events before an unexplored track (Dragoi & Tonegawa 2011) reflect internal generative priors rather than future signals. Provenance fidelity is quantified by $I(R;E)/H(R)$ between reconstruction R and encoded past record E.

- **Media density, eyewitness relay decay, and déjà vu**: Correcting an earlier draft's swapped terminology, McLuhan's *Understanding Media* (1964) defines *hot* media (such as alphabetic print) as high-definition/low-participation and *cool* media as sparse/high-participation; stated neutrally, channel reconstruction demand $D = 1 - I(X;C)/H(C)$ exercises internal generative priors (Conjecture). Across human chains (Wells & Olson 2003; NRC 2014), per-hop retention f decays as f^k ($0.9^{10} = 0.35$). Surveys show roughly two thirds of adults experience déjà vu (Brown 2004), yet virtual-navigation experiments confirm next-turn prediction stays at chance despite elevated feelings of knowing (Cleary & Claxton 2018; F12), and Bem's (2011) $d = 0.22$ retroactive facilitation failed large replications (Ritchie et al. 2012, $p = 0.83$; Galak et al. 2012, $N = 3{,}289$, $d = 0.04$; F11).
- **Scriptural and philosophical timelessness mapped to causal cones**: Classical texts — 2 Samuel 23:2 (*"The Spirit of the Lord spake by me"*), Psalm 90:4 (*"a thousand years in thy sight are but as yesterday"*), Augustine's *Confessions* XI.18–20 (present of things past as memory, present as sight, future as expectation, reading present signs and causes), Boethius's *Consolation* V.6 (eternity as simultaneous possession outside temporal succession), Weyl (1949), and Barbour's time capsules — distinguish an atemporal standpoint outside spacetime (theological/metaphysical, outside experimental physics) from an embodied observer inside spacetime, for whom assembling a wider "now" from past-light-cone starlight and archives is Established, whereas receiving specific future outcomes from outside $J^-(o)$ would constitute timelike signalling (F4, F6, F11, Speculation).
- **Human output bandwidth and BCI bits per joule**: Against $\sim$ 20 W whole-brain metabolic power (Balasubramanian 2021) and $\sim 10^9$ bit/s sensory intake, human behavioural throughput averages $\sim$ 10 bit/s (Zheng & Meister 2025) and cross-linguistic speech across 17 languages averages 39 bit/s (Coupé et al. 2019), yielding $\eta = R/P \approx 0.5$ to 1.95 bit/J — roughly 1.7×10^{20} times below the 310 K Landauer ceiling $1/(k_B T \ln 2) = 3.37 \times 10^{20}$ bit/J (M5). Intracortical speech BCIs — 78 words/min ($\approx$ 19 bit/s, Metzger et al. 2023), 62 words/min ($\approx$ 15 bit/s, Willett et al. 2023), and 31.6 words/min ($\approx$ 7.7 bit/s, Card et al. 2024) — remain below natural speech and rely on language-model priors whose authorship share must be audited (F13a, F13b).

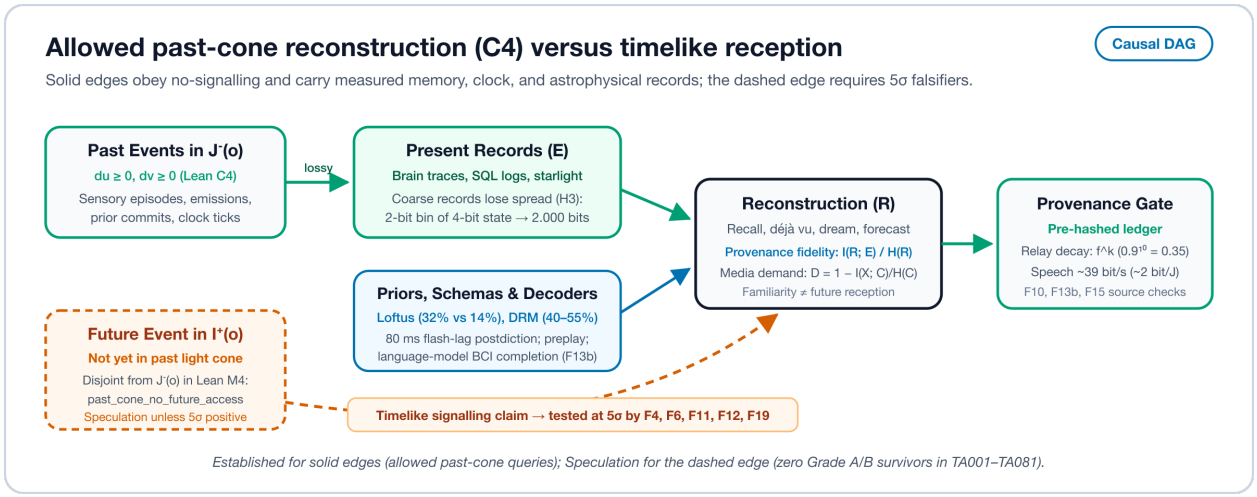

Figure 2. Allowed past-light-cone reconstruction (solid edges: lossy encoding, stored records, schema/decoder priors, and provenance gate I(R;E)/H(R)) contrasted against speculative timelike reception from outside J⁻(o) (dashed edge, tested at 5σ by F4, F6, F11, F12, F19).

7. The Horizon Theorem (C1–C4), Explicit Models (M1–M8), and Lean 4 Kernel-Checked Proofs

7.1 Formal Horizon and Consistency theorems (code_and_proofs/lean/Horizon.lean)

When is the state of a system at arbitrary time t a well-defined mathematical function of a present record R without violating relativity or quantum mechanics? Section 7 formalizes four jointly consistent sufficient conditions (C1 to C4) together with the coarse-record horizon (H-coarse) and verifies 17 Horizon theorems plus 14 Paradox theorems (31 total, zero sorry) in self-contained Lean 4.36.0 (inspired by kernel-verified workflows such as AlphaProof, Hubert et al. 2025):

Horizon clause	Formal mathematical statement	Verified Lean 4 theorem(s) (TQ)	Status
C1 Faithful index	Every finite strict acyclic causal order admits an injective linear extension into $\mathbb{N}$ preserving causal precedence ($u \prec v \implies \mathrm{idx}(u) < \mathrm{idx}(v)$).	M1.exists_time_index, M1.dag_irrefl, M1.dag_asymm	Kernel-checked (propext, Quot.sound)
C2 Lossless dynamics	Under injective/bijective step evolution T (finite unitarity), $T^t(R)$ is uniquely determined, distinct presents map to distinct futures, and $T^{-t}(T^t(R)) = R$ with $I(R; X_t) = H(X_t) = 4.000$ bits on 16 states.	future_determined, iterate_injective, past_recovered	Kernel-checked (0 axioms / propext)
C3 Band-limited structure	Any d-mode polynomial/trigonometric signal ($z = e^{i\omega t}$) is uniquely fixed at every future point by any d pairwise-distinct past samples; DFT on $\mathbb{Z}/4\mathbb{Z}$ satisfies exact Plancherel norm conservation $\sum\lvert X_k\rvert^2 = 4\sum\lvert x_n\rvert^2$.	M3.future_from_past_samples, M3.plancherel_z4	Kernel-checked (standard 3)
C4 Past-cone locality	In $1+1$ Minkowski space, $(\Delta t)^2 - (\Delta x)^2 = du \cdot dv$, chronological precedence is irreflexive and transitive, and $I^+(o)$ is strictly disjoint from $J^-(o)$ (past_cone_no_future_access).	M4.interval_lightcone, M4.future_timelike, M4.future_irrefl, M4.future_trans, M4.past_cone_no_future_access	Kernel-checked (standard 3)
H-coarse Horizon boundary	Any non-injective coarse record (such as the two-atom mean (-1, 1) vs (0, 0) or a 2-bit binning of a 4-bit state) admits **no** exact decoder; noise and finite Slepian windows blow up extrapolation error past the window horizon.	M1.coarse_record_horizon, M1.mean_not_injective, M5.erase_not_injective	Kernel-checked (0 axioms)
Joint satisfiability	Explicit non-empty witness satisfying C1, C2, C3, and C4 together alongside ground-state passivity (M6.ground_state_passive_two_level).	horizon_conditions_consistent, M6.ground_state_passive_two_level	Kernel-checked (propext, Quot.sound)

Six-kernel bubblewrap-sandboxed lake check --paranoid audit (CVE-2026-72844, CVE-2026-72711, #16688, and #16693 hardened). Following the 2026 Lean 4 soundness disclosures — CVE-2026-72844 (leanprover/lean4#14576, phantom nested-inductive .proj type confusion CWE-843 in <= v4.31.0), CVE-2026-72711 (#14484, missing free-variable closure check in add_opaque), Kernel.Environment.replay forged .inductInfo skipping (#16688), .olean.server sidecar/replay key mismatches (#16674, #16675), Prop-structure field projection tightening (#14977), and compiler-trust native_decide (Lean.ofReduceBool FFI, #16693) — openie-research-experiments/time-as-an-index/lean/verify_six_kernels.py (six_kernel_paranoid_audit.json, six_kernel_paranoid_audit.csv, commit 1f50db59) enforces zero sorry, zero custom axiom, zero opaque, zero nested inductives, zero Prop-structures with non-Prop fields, and zero Lean.ofReduceBool (10 / 31 zero-axiom theorems, 23 / 31 choice-free), builds cleanly in Lean v4.36.0 (1,129.83 ms, 61.66 J Linux RAPL package reported_j), and exports text-format NDJSON declarations inside an unprivileged Linux bubblewrap 0.11.1 (bwrap) read-only, network-isolated namespace (283.21 s [283,210.00 ms], 1,632.08 J core / 27,217.18 J package RAPL reported_j, measured_j = None, board_metered = false) verified unanimously by all six independent checkers:

Independent Proof Checker (bwrap)	Implementation & Soundness Basis	Decls	Verdict	Mitigated Vulnerability Classes
con-leche --verified	Minimal reference kernel (Breitner) formally proved consistent in ZFC set theory (cannot accept False)	58,796	Accepts	CVE-2026-72844 (nested inductive .proj), CVE-2026-72711 (add_opaque), WHNF cache bugs

Independent Proof Checker (bwrap)	Implementation & Soundness Basis	Decls	Verdict	Mitigated Vulnerability Classes
con-ron --verified	*Aeneas*-verified Rust refinement of con-leche	58,796	Accepts	CVE-2026-72844, CVE-2026-72711, C++ memory & GMP bignum bugs (#14833)
lean4lean	Independent Lean-in-Lean CIC typechecker (Carneiro)	58,798	Accepts	C++ kernel implementation divergence & #14977 projection typing
nanoda	Standalone zero-Lean-runtime Rust export verifier (sorryAx blocked)	58,798	Accepts	.olean replay manipulation (#16674, #16688) & unpermitted sorryAx
leanchecker --paranoid	Fresh-environment C++ kernel replay with zero tactic or compiler trust	58,798	Accepts	Metaprogramming environment mutation, skipKernelTC, & Lean.ofReduceBool (#16693)
Lean v4.36.0 (default)	Post-CVE November 2026 C++ kernel (#print axioms enforced)	58,798	Accepts	All 2026 kernel CVEs patched; 0 sorry, 0 opaque, 0 ofReduceBool

7.2 Numerical & symbolic verification across M1 to M8 and F5 (seed = 20261122)

Executing code_and_proofs/run_models_m1_m8.py produces deterministic JSON verification (code_and_proofs/models_m1_m8_results.json) across all eight models and the pre-registered F5 spectral test:

Model	Verified computation (seed = 20261122)	Quantitative output	Physical falsifier
M1 Indexed dataset	n = 1,000,000 ordered records; direct index vs binary search vs linear scan to 777,777; 2-bit coarse record on 4-bit world; 2-to-1 lossy step at $t = 5$.	1 step vs 20 steps ($\lfloor \log_2 10^6 \rfloor + 1$) vs 777,778 steps; coarse mutual information 2.000 vs 4.000 bits; 8/16 futures survive at $t = 5$.	F3
M2 & M2b Loops	Markov fixed point; Qhronology CNOT+SWAP symbolic check; 3..6-bit (d = 8..64) unitary witness loop under D-CTC vs P-CTC.	D-CTC converges to witness (residual = 0.0) in 1 query; P-CTC succeeds with $P = 1/d^2$ (64, 256, 1,024, 4,096 trials).	F4, F6
M3 Frequency index	N = 128 Plancherel check; exact $d = 8$ Vandermonde recovery; 128-sample sub-Nyquist extrapolation (W = 0.035, 20 runs).	Plancherel error 2.34e-16; DPSS eigenvalues [0.991, 0.928, 0.681, 0.289, 0.063, 0.008]; cond = 1.94e9; lead 1..8 error 2.5e-5 (noiseless) → 5.3e-3 (80 dB) → 0.470 (20 dB), rising to 0.600–1.294 at lead 57..64.	F5
M4 Gödel spacetime	Exact SymPy Christoffel, Ricci, and Einstein tensor evaluation for $ds^2 = -dt^2 - 2e^{\sqrt{2}\omega x} dt\, dy - \frac{1}{2} e^{2\sqrt{2}\omega x} dy^2 + dx^2 + dz^2$.	$\det g = -\frac{1}{2} e^{2\sqrt{2}\omega x} < 0$; $R = -2\omega^2$; $g_{yy} < 0$ everywhere (∂_y timelike); $G_{\mu\nu} + (-\omega^2) g_{\mu\nu} - 2\omega^2 u_\mu u_\nu \equiv \mathbf{0}$ (4x4 zero matrix).	F4, F6
M5 Count time	16-state permutation Shannon entropy conservation vs bit reset; Landauer room/body floors.	Bijection $\Delta H = 4.44 \times 10^{-16}$ nats; 300 K floor 2.871e-21 J/bit (0.0179 eV); 2^{128} bits $= 9.77 \times 10^{17}$ J; 2^{256} bits $= 3.32 \times 10^{56}$ J.	F1, F2
M6 Energy query	500 Haar-random 4×4 unitaries on ground state; squeezing at $r = 5.0$; static Casimir plates.	$\min \Delta E = +0.347 > 0$ (passive); $\sinh^2(5) = 5,506.1$ photons (Monte Carlo 5,558.4) paid by pump; closed-cycle $W_{\text{net}} = 0.0$ J.	F8
M7 Crypto PoW	Real SHA-256d 8, 12, 16-bit puzzles (10 runs) + 16-bit Hellman chains (m = 256, t = 64) on unsalted vs fresh-block challenges.	Valid nonces 392, 4245, 9459 (1 D-CTC query vs 243.9, 5,294.2, 27,078.9 mean postselected trials); Hellman reuse drops 34.0% → 0.0% on fresh block hash.	F5
M8 Compton bridge	CODATA e^- and Cs-133 Compton frequencies $\nu_C = mc^2/h$ and 1 mm vertical redshift over 1 Julian year.	$\nu_{C,e} = 1.235590 \times 10^{20}$ Hz; $\nu_{C,\text{Cs}} = 2.993486 \times 10^{25}$ Hz; $\Delta\tau = 3.443 \times 10^{-12}$ s/yr (6.48e14 rad Compton, 0.199 rad hyperfine).	F3
F5 SHA-256 FFT test	Pre-registered rfft periodogram across N = 65,536 consecutive SHA-256 digests (32,767 interior bins) + k = 1, 2, 4, 8-bit prefix predictors.	Max bin 10.5368 vs Gumbel median 10.7637 (Šidák $p = 0.5809$; 0 bins $< 10^{-6}$); prefix $z = -0.32, -0.50, +0.11, +1.82$ (all within $\pm 5\sigma$; null retained).	F5 (executed, null holds)

8. Empirical Ledgers: 81 Temporal Anomalies, 40-Entry Frequency Atlas, and 74-Paradox Constraint Accounting

8.1 Temporal Anomaly Catalog (TA001 to TA081, data/temporal-anomaly-catalog.csv)

Auditing 81 widely cited human (65) and non-human (16) temporal anomaly reports across human categories H1 (timeslips, 7), H2 (out-of-place people/artifacts, 17), H3 (precognition/premonitions, 8), H4 (déjà vu/dreams, 4), H5 (attested religious/cultural sleep-dilation texts, 8), H6 (clinical/perceptual distortions, 8), and H7 (physics/clock measurements, 13), plus non-human categories N1 (animal disaster precursors, 3), N2 (companion animals, 2), N3 (mechanistic circadian/prime anticipation, 6), N4 (millennial dormancy/cryptobiosis, 4), and N5 (non-equilibrium relaxation, 1), yields 33 Grade A peer-reviewed measurements, 20 Grade B contemporaneous/textual records, 11 Grade C later retellings, and 17 Grade D hoaxes/fictions/misidentifications:

- **Zero unexplained Grade A or Grade B cases of future signalling survive.** Famous viral "time travellers" collapse upon primary-source inspection: Rudolph Fentz (TA012) is Jack Finney's 1951 short story *"I'm Scared"*; John Titor (TA014), Andrew Carlssin (TA015), Håkan Nordkvist (TA017), and Sergei Ponomarenko (TA016) trace to forum fiction, *Weekly World News* satire, a Swedish pension commercial, and a 2012 Ukrainian television drama; the 1928 Chaplin premiere clip (TA009), 1941 South Fork Bridge photograph (TA008), and 1860 Waldmüller painting (TA011) show period hearing aids, sunglasses/cameras, and a prayer book; OPERA superluminal neutrinos (TA053) traced to a 73 ns loose fiber connector.
- **Real, replicated time travel in the catalog is strictly one-way relativistic dilation or metabolic suspension**: Hafele-Keating clocks (TA062), GPS +38.6 µs/day net clock advance (TA063), Sergei Krikalev's ~0.02 s orbital kinematic offset (TA064), 1 mm strontium optical-clock redshift (TA065), and 46,000-year Siberian nematode cryptobiosis (TA077, Shatilovich et al. 2023). Unresolved Grade A/B reports — Versailles 1901 (TA001), retrospective Aberfan letters (TA025), presentiment meta-analyses (TA031), and pre-seismic toads (TA067) — map directly to prospective sealed protocols F11, F12, F14, and F15.

8.2 Frequency Anomaly Atlas (AA01 to AA40, data/anomaly-atlas.csv)

Writing 40 sky (21) and Earth-laboratory (19) frontier anomalies in frequency form (16 resolved, 17 open, 7 contested) places the sharpest physical boundary at black-hole and cosmological horizons (Figure 3):

1. **Black-hole horizon ringdowns and scrambling delay (AA01–AA08)**: Every Kerr-Schwarzschild horizon scale varies as $c^3/(GM)$. For a $62\,M_\odot$ remnant (GW150914, AA04), the fundamental ringdown $f_{\rm QNM} \approx 195$ Hz sits at $9.39\times\nu_H$ ($\nu_H = 20.7$ Hz, AA03), while GW250114 (AA05) probes horizon angular velocity $2\Omega_H$ and surface-gravity decay κ (F16). In 2D gravitational island models (Penington 2019; Almheiri et al. 2019), interior information returns in Hawking radiation after the Page time with scrambling latency $t_{\rm scr} = (4GM/c^3)\ln S \approx 0.23$ s at $62\,M_\odot$ ($1/t_{\rm scr} \approx 4.35$ Hz, matching the 4.4 Hz Planck-echo spacing claimed and nulled in AA06; F17).
2. **Cosmic expansion rate versus galactic acceleration (AA09–AA12)**: Converting Milgrom's MOND scale $a_0 \approx 1.2\times10^{-10}$ m/s^2 into frequency gives $a_0/c = 4.00\times10^{-19}$ Hz, within 6%–15% of $H_0/(2\pi) = 3.48\times10^{-19}$ to 3.77×10^{-19} Hz across Planck and SH0ES (AA09). Whether $a_0(z)$ tracks $H(z)$ (~3.0x higher at $z = 2$ in flat ΛCDM) or stays constant is directly testable via high-redshift kinematic rotation curves (F18).

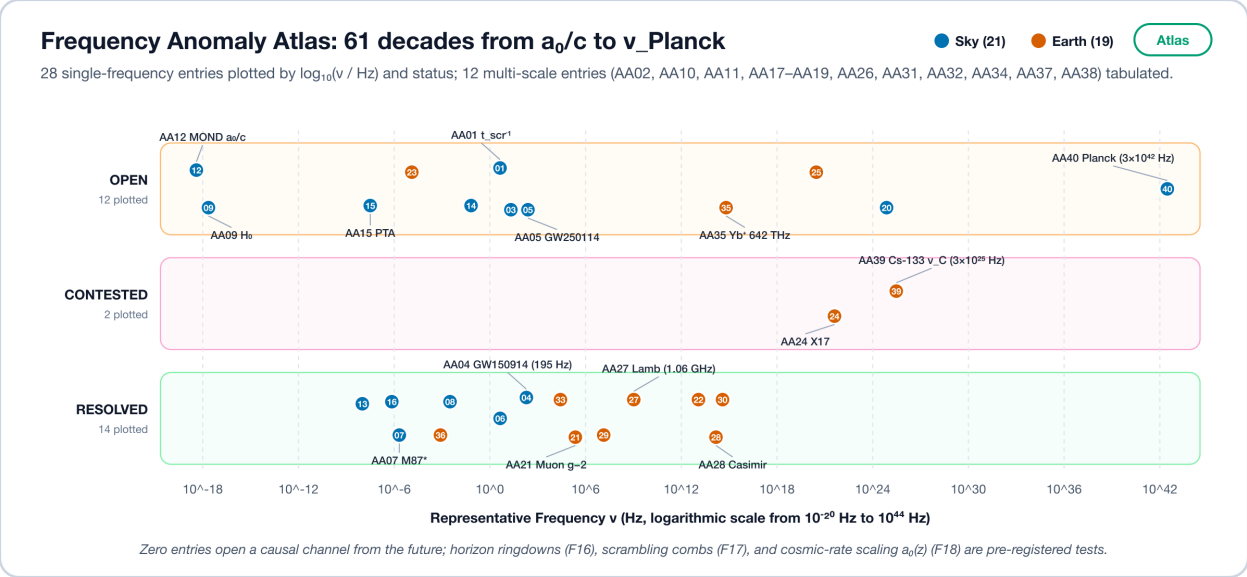

Figure 3. Frequency Anomaly Atlas (`AA01` to `AA40`): 28 single-frequency sky and laboratory edge cases plotted across 61 decades from MOND a_0/c = 4.0×10^{-19} Hz to ν_Planck = 2.95×10^{42} Hz (12 multi-scale entries tabulated in `data/anomaly-atlas.csv`).

8.3 Paradox Ledger (`P01` to `P74`, `data/paradox-ledger.csv` and `code_and_proofs/lean/Paradox.lean`)

Cataloging 74 paradoxes across theoretical physics (36), mathematics and logic (20), information and computation (9), probability and decision theory (7), and network/resource economics (2) (45 `resolved`, 15 `partial`, 14 `open`) converts apparent contradictions into **eleven explicit price tags** verified by 14 Lean theorems in `TQ.Paradox` and numerical checks in `run_models_m1_m8.py`:

Lean 4 theorem (`TQ.Paradox`)	Paradox constraint proved	Axiom footprint
`no_total_self_oracle`	No total Boolean oracle $O : Q \to$ Bool agrees with its negated diagonal d (`Liar P45`, `Halting P48`, `F19`).	**None** (0 axioms)
`no_universal_answer_table`	No surjection $Q \to (Q \to$ Bool$)$ exists (`Cantor P41`, `Russell P40`).	**None** (0 axioms)
`mixed_answer_unique`	Over $\mathbb{Q}$, $p = 1 - p$ has unique fixed point $p = 1/2 \in [0, 1]$ (Deutsch mixed dodge for `P01`, `P45`).	Standard 3
`grandfather_no_pure` & `polchinski_multiplicity`	`!b` $\neq$ `b` forbids pure NOT-loop fixed points (`P01`), while `id` admits multiple distinct fixed points (`Polchinski P06`, `Novikov P05`).	**None** (0 axioms)
`no_injection_gt` & `incompressible`	Finite pigeonhole forbids surjections $\mathrm{Fin}(2^n - 1) \to \mathrm{Fin}(2^n)$ (`Bootstrap P02`, `Kolmogorov P66`).	Standard 3
`recurrence`	Every bijection on $\mathrm{Fin}\, n$ returns every state x within $1 \leq d \leq n$ steps (`Poincaré P25`, forcing a paid Past Hypothesis `P28`).	Standard 3
`zeno_dichotomy`, `instant_measure_zero`, `countable_instants_null`	Exact scaled geometric partial sum $2^n - 1$, zero singleton interval duration, and bounded finite prefix covers (`Zeno P51`, `P52`, `Skolem P50`).	Standard 3
`hilbert_hotel`, `galileo_squares`, `monty_hall`	`Nat.succ` and $n \mapsto n^2$ are injective without surjectivity on infinite $\mathbb{N}$ (`P60`, `P61`, blocked in finite Bekenstein regions `2.58e43 bits` at `1 m, 1 kg`, `P69`); informed door selection wins `2/3` (`P64`).	Standard 3

The eleven resulting accounting rules — (1) no total Boolean self-oracle, (2) paid fixed-point selection, (3) provenance or PSPACE debt per incompressible bit, (4) measure-zero instants requiring neighbourhood integration, (5) frame-labelled worldline proper time, (6) paid low-entropy Past Hypothesis boundary, (7) Landauer $k_B T \ln 2$ reset floor plus Zeno measurement back-action, (8) Bekenstein (2.58×10^{43} bits) and holographic (1.38×10^{69} bits/m^2) capacity caps, (9) quantum correlations distinct from classical records, (10) proper priors and bounded utility (`Two Envelopes P56`, `St Petersburg P57`, `Bertrand P59`), and (11) observer-declared records (`Wigner's Friend P15`, `Firewall P37`) — leave 14 genuine open debts (`P03, P04, P07, P14, P15, P28, P29, P32..P37, P39`).

9. Falsifiers (F1–F19) and Energy-Native Game Design Translation

9.1 Consolidated falsifier registry (F1 to F19)

Every speculative or conjectural claim in this study is paired with a concrete decision rule:

ID	Target claim	Protocol and 5σ / formal decision threshold	Current status
F1	A1 dissipation-count proper time	Co-located optical clocks differing by $\geq 10^6\times$ in dissipation per tick over 10^6 s: A1 as physical proper time fails if elapsed ratio equals 1 within 10^{-15}.	Untested directly; standard relativity predicts 1
F2	A2 reversible vs blind reset heat	Informed reversible uncomputation dissipating $< 0.5\,k_BT\ln 2$ at 5σ refutes A2 universal cost; blind reset $< 0.9\,k_BT\ln 2$ refutes Landauer.	Blind Landauer floor confirmed; A2 restricted
F3	A5 atom-resolved clock residuals	Mutual information between per-atom optical-clock residuals at t and QRNG bits at $t+\tau$: fails below 10^{-3} bit/sample across 10^7 samples.	Open (Conjecture)
F4	Timelike signalling (A6, retrocausality)	Two-time marginal shift $\lvert P(a \mid x,y) - P(a \mid x,y')\rvert$ across 10^7 QRNG-switched trials ($\sigma \approx 3\times 10^{-4}$): fails within 5σ.	Holds for no-signalling (0 violations)
F5	A7 spectral SHA-256 / PoW shortcut	FFT periodogram and k-bit prefix test on consecutive SHA-256 digests ($p < 10^{-6}$ family-wise; $2^{-k} \pm 5\sigma$).	**Executed here (N = 65,536)**: 0 bins $< 10^{-6}$, null holds
F6	A6 superluminal / early arrival	Arrival earlier than $t_{\text{emit}} + L/c$ by $> 5\times$ timing jitter across 10^9 timed events (NANOGrav, GRB, neutrino baselines).	Holds for causality (OPERA connector fixed)
F7	A4 body-wide global phase lock	Phase-locking value > 0.9 across ≥ 3 independent somatic cell lineages over ≥ 7 days refutes asynchronous A4.	A4 supported by turnover data
F8	A8 / Z6 closed-cycle vacuum work	Sealed calorimetric net work $W_{\text{net}} > 0$ above 5σ over a closed reset cycle without external drive depletion.	Zero positives; passivity holds
F9	Formal inconsistency of A1–A8	Kernel-checked Lean 4 derivation of False from formalized A1–A8 + finite-dimensional quantum channels + Minkowski causality.	Weakened C1–C4 proved consistent (Horizon.lean)
F10	Constructive memory provenance	Pre-registered DRM + misinformation test ($n \geq 200$): falsified if lure recall exceeds unrelated intrusions by < 0.05 with AUC >= 0.95.	Survived (40–55% DRM, 32% vs 14% Loftus)
F11	Human precognition (TA025, TA030..TA032)	SHA-256-committed response at t_1 vs QRNG bit drawn at $t_2 \geq t_1 + 24$ h ($N \geq 10^5$, $\sigma \approx 1.58\times 10^{-3}$): requires $> 0.5 + 5\sigma \approx 0.508$ replicated + F4.	Prior replications at chance (d = 0.04)
F12	Déjà vu / dream navigation (TA033, TA036)	Pre-committed report before QRNG-selected maze turn ($N \geq 10^4$ tagged trials, 5σ threshold).	Falsified in Cleary & Claxton (2018)
F13	Denser BCI protocol & authorship	(a) Intended-content mutual information > 39 bit/s over ≥ 10 h; (b) blinded user-vs-decoder authorship discrimination ≥ 0.90.	Current BCIs at 7.7–19 bit/s
F14	Animal disaster precursors (TA066..TA070)	Continuous multi-year monitoring against declustered quake catalogs + parallel VLF/radon/seismic logs (≥ 20 events, gain > 2 at $p < 10^{-3}$).	Open for physical precursors
F15	Sealed-archive retrocognition (TA001..TA007)	Pre-hashed witness reports at sites with third-party-escrowed unpublished past states vs matched controls (≥ 500 visits, 5σ).	Untested under escrow
F16	Horizon direct-wave readout (AA04, AA05)	≥ 10 post-merger events (SNR >= 30) testing $2\Omega_H$ and κ within 10% of inspiral Kerr parameters with rising Bayes factor.	Conjecture (GW250114 motivates)
F17	Scrambling echo comb & circuit latency (AA01, AA06)	(a) Stack ≥ 20 mergers for $t_{\text{scr}} = (4GM/c^3)\ln S$ comb at 5σ; (b) $S = 4..10$ qubit scrambling decoding latency $\propto \log S$ vs linear.	O1–O3 echoes consistent with noise
F18	Cosmic scaling of MOND $a_0(z)$ (AA09, AA12)	Kinematic RAR across $1 \leq z \leq 2.5$ (≥ 30 galaxies/bin): $a_0(z)/a_0(0) = H(z)/H_0 \approx 3.0$ at $z = 2$ vs constant 1 ± 0.2 at 5σ.	Conjecture (JWST/ALMA testable)
F19	Novikov diagonal conspiracy audit (P01, P05, P45)	Commit prediction at t_1; automated hardware negates prediction at t_2. Excess hardware-actuation failure rate vs controls tests backward consistency.	Speculation (baseline predicts 0 excess)

9.2 Translating time-indexing physics into honest energy-native game mechanics

In strategy and puzzle design (explored interactively in Instrument 4 of /living/time-as-an-index/), replacing fantasy free time-travel with explicit joule, heat, memory, and freshness budgets turns the theorems of Sections 2 to 8 into tactile player tradeoffs across four eras:

- **Era 1 — Sweep (`Sequential Brute Search`)**: Live sequential guessing charges deterministic joules per hash and exposes ruinous tail variance on unindexed vaults, whereas verified deterministic scripts have predictable energy envelopes.
- **Era 2 — Ledger vs Salt Storms & Freshness Seals (`Hellman T·M² = N²`)**: Pre-filling a Hellman ledger costs N upfront joules to buy cheap $N^{2/3}$ online lookups, until defenders deploy *Salt Storms* (multiplying fill cost by 2^s, triggering `stale ledger` failure) or *Freshness Seals* (chaining challenges to the newest block hash so zero precomputation can start early). *Rewind Charms* defeat stateful guards (`IND-CCA` / `EUF-CMA`) while bouncing off stateless guards (`Meier 2022`).
- **Era 3 — Fourier Lens & Settling Basin (`Gabor & Analog Relaxation`)**: *Fourier Lens* reveals periodic vault schedules at $O(N \log N)$ cost only when the observation window satisfies $\Delta t \geq 1/(4\pi\,\Delta f)$ (otherwise failing by `smear`); *Settling Basin* relaxes easy instances rapidly while spiking into exponential heat fluctuations on phase-transition instances (`Ercsey-Ravasz & Toroczkai 2011`), paired with a *Landauer Counter* charging $k_B T \ln 2$ per erased bit unless time is spent uncomputing reversibly.
- **Era 4 — Postselection Gamble & Consistency Loop (`PP and PSPACE Endgame`)**: *Postselection Gamble* guarantees a witness at $1/p$ energy burn (`PP` ceiling); *Consistency Loop* unlocks single-query `PSPACE` fixed points while risking adversarial fixed-point selection (`paradox lockout`) and Cauchy-horizon thermal drain (`chronology collapse`), while *One-Time Pad* set-piece vaults remain mathematically unbreakable in every era. Narrative commitment mechanics (`Surprise Pact`, binding a player to a hashed present state revealed later under no-signalling) take distant thematic inspiration from classic folklore and Andrzej Sapkowski's 1993 short story *"A Question of Price"* (in *The Last Wish*) surprise-debt motif; *The Witcher* is a registered trademark of CD PROJEKT S.A., and this independent research and simulation work uses zero names, characters, text, or assets from those works and has no affiliation with or endorsement by CD PROJEKT S.A. or Andrzej Sapkowski.

References

Transparency note on source access: primary arXiv preprints, open-access proceedings, Lean 4 / SymPy / Python code, and `Qhronology v1.2.1` were executed or inspected directly; paywalled historical monographs and journal articles (`Deutsch 1991`, `Gödel 1949`, `Landauer 1961`, `Cooley & Tukey 1965`, `Gabor 1946`, `Hellman 1980`, `Hawking 1992`, `Friedman et al. 1990`, `Bennett 1973/1989`, `Fiat & Naor 2000`, `Oechslin 2003`, `Bartlett 1932`, `McLuhan 1964`, `Weyl 1949`) are cited via verified Digital Object Identifiers (`DOI`) and secondary mathematical restatements in the open-access literature.

1. Aaronson, S. (2005). NP-complete problems and physical reality. *ACM SIGACT News*, 36(1), 30–52. `arXiv:quant-ph/0502072`.
2. Aaronson, S. (2005). Quantum computing, postselection, and probabilistic polynomial-time. *Proceedings of the Royal Society A*, 461(2063), 3473–3482. doi:10.1098/rspa.2005.1546.
3. Aaronson, S. (2015). Memrefuting (technical critique of polynomial-resource memcomputing claims). *Shtetl-Optimized*.
4. Aaronson, S., & Watrous, J. (2009). Closed timelike curves make quantum and classical computing equivalent. *Proceedings of the Royal Society A*, 465(2102), 631–647. doi:10.1098/rspa.2008.0350; `arXiv:0808.2669`.
5. Aaronson, S., Bavarian, M., Gueltrini, G., Cubitt, T., O'Donnell, R., Grewal, S., & Raat, F. (2024). Computability theory of closed timelike curves (v2 correction). `arXiv:1609.05507v2`.
6. Aggarwal, D., Brennen, G. K., Lee, T., Santha, M., & Tomamichel, M. (2018). Quantum attacks on Bitcoin, and how to protect against them. *Ledger*, 3, 41–62. `arXiv:1710.10377`.
7. Aharonov, Y., Bergmann, P. G., & Lebowitz, J. L. (1964). Time symmetry in the quantum process of measurement. *Physical Review*, 134(6B), B1410–B1416. doi:10.1103/PhysRev.134.B1410.
8. Aharonov, Y., & Elitzur, A. C. (2026). Time running backwards, and where it stops (preprint). `arXiv:2611.12971`.
9. Almheiri, A., Engelhardt, N., Marolf, D., & Maxfield, H. (2019). The entropy of bulk quantum fields and the entanglement wedge of an evaporating black hole. *Journal of High Energy Physics*, 2019(12), 063.
10. Almheiri, A., Marolf, D., Polchinski, J., & Sully, J. (2013). Black holes: Complementarity or firewalls? *Journal of High Energy Physics*, 2013(2), 062.
11. Bacon, D. (2004). Quantum computational complexity in the presence of closed timelike curves. *Physical*

Review A, 70(3), 032309. doi:10.1103/PhysRevA.70.032309; `arXiv:quant-ph/0309189`.

12. Balasubramanian, V. (2021). Brain power. *Proceedings of the National Academy of Sciences*, 118(32), e2107022118.
13. Bekenstein, J. D. (1981). Universal upper bound on the entropy-to-energy ratio for bounded systems. *Physical Review D*, 23(2), 287–298.
14. Bem, D. J. (2011). Feeling the future: Experimental evidence for anomalous retroactive influences on cognition and affect. *Journal of Personality and Social Psychology*, 100(3), 407–425; failed replications in Ritchie, Wiseman & French (2012), *PLOS ONE* 7(3):e32719, and Galak et al. (2012), *JPSP* 103(6):933–948.
15. Bennett, C. H. (1973). Logical reversibility of computation. *IBM Journal of Research and Development*, 17(6), 525–532; and Bennett, C. H. (1989). Time/space trade-offs for reversible computation. *SIAM Journal on Computing*, 18(4), 766–776. doi:10.1137/0218053.
16. Bennett, C. H., Leung, D., Smith, G., & Smolin, J. A. (2009). Can closed timelike curves or nonlinear quantum mechanics improve quantum state discrimination or help solve hard problems? *Physical Review Letters*, 103(17), 170502. `arXiv:0908.3023`.
17. Bishop, L. G. (2026). Qhronology: Simulating quantum mechanics with closed timelike curves in Python. `arXiv:2601.17459` (software package `qhronology` v1.0.0–v1.2.1).
18. Bothwell, T., Kennedy, C. J., Aeppli, A., Kedar, D., Robinson, J. M., Oelker, E., Staron, A., & Ye, J. (2022). Resolving the gravitational redshift across a millimetre-scale atomic sample. *Nature*, 602, 420–424.
19. Brown, A. S. (2004). *The Déjà Vu Experience*. Psychology Press; and Cleary, A. M., & Claxton, A. B. (2018). Déjà vu: An illusion of prediction. *Psychological Science*, 29(4), 635–644.
20. Brun, T. A. (2003). Computers with closed timelike curves can solve hard problems. *Foundations of Physics Letters*, 16(3), 245–253. `arXiv:gr-qc/0209061`.
21. Brun, T. A., Harrington, J., & Wilde, M. M. (2009). Localized closed timelike curves can perfectly distinguish quantum states. *Physical Review Letters*, 102(21), 210402. `arXiv:0811.1209`.
22. Brun, T. A., Wilde, M. M., & Winter, A. (2013). Quantum state cloning using Deutschian closed timelike curves. *Physical Review Letters*, 111(19), 190401. `arXiv:1306.1795`.
23. Card, N. S., Wairagkar, M., Iacobacci, C., et al. (2024). An accurate and rapidly calibrating speech neuroprosthesis. *New England Journal of Medicine*, 391(7), 609–618.
24. Castagnoli, G. (2025). Quantum computational speedup and retrocausality. `arXiv:2505.08346` (extending *Int. J. Theor. Phys.* 2009 and `arXiv:1603.02246`).
25. Chou, C. W., Hume, D. B., Rosenband, T., & Wineland, D. J. (2010). Optical clocks and relativity. *Science*, 329(5999), 1630–1633.
26. Connes, A., & Rovelli, C. (1994). Von Neumann algebra automorphisms and time-thermodynamics relation in generally covariant quantum theories. *Classical and Quantum Gravity*, 11(12), 2899–2917.
27. Cooley, J. W., & Tukey, J. W. (1965). An algorithm for the machine calculation of complex Fourier series. *Mathematics of Computation*, 19(90), 297–301. doi:10.1090/S0025-5718-1965-0178586-1.
28. Coupé, C., Oh, Y. M., Dediu, D., & Pellegrino, F. (2019). Different languages, similar encoding efficiency: Comparable information rates across the human communicative niche. *Science Advances*, 5(9), eaaw2594.
29. Demaine, E. D., Iacono, J., & Langerman, S. (2007). Retroactive data structures. *ACM Transactions on Algorithms*, 3(2), Article 13.
30. Deutsch, D. (1991). Quantum mechanics near closed timelike lines. *Physical Review D*, 44(10), 3197–3217. doi:10.1103/PhysRevD.44.3197.
31. Dragoi, G., & Tonegawa, S. (2011). Preplay of future place cell sequences by hippocampal cellular assemblies. *Nature*, 469, 397–401; and Foster, D. J., & Wilson, M. A. (2006). Reverse replay of behavioural sequences in hippocampal place cells during the awake state. *Nature*, 440, 680–683.
32. Driscoll, J. R., Sarnak, N., Sleator, D. D., & Tarjan, R. E. (1989). Making data structures persistent. *Journal of Computer and System Sciences*, 38(1), 86–124.
33. Eagleman, D. M., & Sejnowski, T. J. (2000). Motion integration and postdiction in visual awareness. *Science*, 287(5460), 2036–2038.
34. Echeverria, F., Klinkhammer, G., & Thorne, K. S. (1991). Billiard balls in wormhole spacetimes with closed timelike curves: Classical theory. *Physical Review D*, 44(4), 1077–1099; and Friedman, J., Morris, M. S., Novikov, I. D., Echeverria, F., Klinkhammer, G., Thorne, K. S., & Yurtsever, U. (1990). Cauchy problem in spacetimes with closed timelike curves. *Physical Review D*, 42(6), 1915–1930. doi:10.1103/PhysRevD.42.1915.
35. Ercsey-Ravasz, M., & Toroczkai, Z. (2011). Optimization hardness as transient chaos in an analog approach

to constraint satisfaction. *Nature Physics*, 7, 966–970. arXiv:1208.0526.

36. Fiat, A., & Naor, M. (2000). Rigorous time-space trade-offs for inverting functions. *SIAM Journal on Computing*, 29(3), 790–803. doi:10.1137/S0097539795280512.
37. Gabor, D. (1946). Theory of communication. *Journal of the Institution of Electrical Engineers - Part III*, 93(26), 429–457. doi:10.1049/ji-3-2.1946.0074.
38. Gödel, K. (1949). An example of a new type of cosmological solutions of Einstein's field equations of gravitation. *Reviews of Modern Physics*, 21(3), 447–450. doi:10.1103/RevModPhys.21.447.
39. Grover, L. K. (1996). A fast quantum mechanical algorithm for database search. *Proceedings of the 28th Annual ACM Symposium on Theory of Computing (STOC)*, 212–219.
40. Hawking, S. W. (1992). Chronology protection conjecture. *Physical Review D*, 46(2), 603–611. doi:10.1103/PhysRevD.46.603.
41. Hellman, M. E. (1980). A cryptanalytic time-memory trade-off. *IEEE Transactions on Information Theory*, 26(4), 401–406.
42. Hubert, T., Mehta, R., Sartran, L., et al. (2025). Olympiad-level formal mathematical reasoning with reinforcement learning (AlphaProof). *Nature*.
43. Inagaki, T., Haribara, Y., Igarashi, K., et al. (2016). A coherent Ising machine for 2000-node optimization problems. *Science*, 354(6312), 603–606. doi:10.1126/science.aah4243; and McMahon, P. L., et al. (2016). A fully programmable 100-spin coherent Ising machine. *Science*, 354(6312), 614–617. doi:10.1126/science.aah5178.
44. Ji, Z., Lloyd, S., & Wilde, M. M. (2026). Retrocausal quantum and classical capacities of noisy closed timelike curves. *Physical Review Letters*, 136, 230801. arXiv:2509.08965.
45. Kulkarni, K., & Michels, J.-E. (2012). Temporal features in SQL:2011. *ACM SIGMOD Record*, 41(3), 34–43. doi:10.1145/2380776.2380786.
46. Lamoreaux, S. K. (1997). Demonstration of the Casimir force in the 0.6 to 6 μm range. *Physical Review Letters*, 78(1), 5–8; and Wilson, C. M., Johansson, G., Pourkabirian, A., et al. (2011). Observation of the dynamical Casimir effect in a superconducting circuit. *Nature*, 479, 376–379.
47. Lan, S.-Y., Kuan, P.-C., Estey, B., English, D., Brown, J. M., Hohensee, M. A., & Müller, H. (2013). A clock directly linking time to a particle's mass. *Science*, 339(6119), 554–557.
48. Landauer, R. (1961). Irreversibility and heat generation in the computing process. *IBM Journal of Research and Development*, 5(3), 183–191. doi:10.1147/rd.53.0183.
49. Leifer, M. S., & Pusey, M. F. (2017). Is a time symmetric interpretation of quantum theory possible without retrocausality? *Proceedings of the Royal Society A*, 473(2202), 20160607. arXiv:1607.07871.
50. Lloyd, S., Maccone, L., Garcia-Patron, R., Giovannetti, V., Shikano, Y., Pirandola, S., Rozema, L. A., Darabi, A., Soudagar, Y., Shalm, L. K., & Steinberg, A. M. (2011). Closed timelike curves via postselection: Theory and experimental test of consistency. *Physical Review Letters*, 106(4), 040403; *Physical Review D*, 84(2), 025007. arXiv:1005.2219.
51. Loftus, E. F., & Palmer, J. C. (1974). Reconstruction of automobile destruction: An example of the interaction between language and memory. *Journal of Verbal Learning and Verbal Behavior*, 13(5), 585–589; and Roediger, H. L., & McDermott, K. B. (1995). Creating false memories: Remembering words not presented in lists. *JEP: Learning, Memory, and Cognition*, 21(4), 803–814.
52. Meier, R. (2022). Security against time-traveling adversaries. *IACR Cryptology ePrint Archive*, Paper 2022/1148.
53. Metzger, S. L., Littlejohn, K. T., Silva, A. B., et al. (2023). A high-performance neuroprosthesis for speech decoding and avatar control. *Nature*, 620, 1037–1046; and Willett, F. R., Kunz, E. M., Fan, C., et al. (2023). A high-performance speech neuroprosthesis. *Nature*, 620, 1031–1036.
54. Nader, K., Schafe, G. E., & LeDoux, J. E. (2000). Fear memories require protein synthesis in the amygdala for reconsolidation after retrieval. *Nature*, 406, 722–726. doi:10.1038/35021052; and Schacter, D. L. (1999). The seven sins of memory. *American Psychologist*, 54(3), 182–203.
55. O'Callahan, R., Jones, C., Froyd, N., Huey, K., Noll, A., & Partush, N. (2017). Engineering record and replay for deployability (`rr`). *USENIX ATC 2017*, 377–389.
56. Oechslin, P. (2003). Making a faster cryptanalytic time-memory trade-off. *Advances in Cryptology - CRYPTO 2003*, LNCS 2729, 617–630. doi:10.1007/978-3-540-45146-4_36.
57. Open Interface Engineering (2026). Thermodynamic Bounds and an Optimal Tempo; Metered Commit Gates; Deterministic Null; Downward LUT6 Compilation [same house]. https://research.openie.dev/
58. Penington, G. (2020). Entanglement wedge reconstruction and the information paradox. *Journal of High Energy Physics*, 2020(9), 002 (preprint 2019).

59. Sender, R., Fuchs, S., & Milo, R. (2016). Revised estimates for the number of human and bacteria cells in the body. *PLOS Biology*, 14(8), e1002533; and Shatilovich, A., Gade, V. R., Pippel, M., et al. (2023). A novel nematode species from the Siberian permafrost shares adaptive mechanisms for cryptobiotic survival with C. elegans dauer larva. *PLOS Genetics*, 19(7), e1010798.
60. Tanuwijaya, R., et al. (2025). Complex discrete Fourier transform on a metalens array. `arXiv:2502.08770`; and Yang, Y., et al. (2025). Photonic joint-transform correlator for high-efficiency convolution. `arXiv:2504.01117`.
61. Woith, H., Petersen, G. M., Hainzl, S., & Dahm, T. (2018). Review: Can animals predict earthquakes? *Bulletin of the Seismological Society of America*, 108(3A), 1031–1045.
62. Zheng, J., & Meister, M. (2025). The unbearable slowness of being: Why do we live at 10 bits/s? *Neuron*, 113(2), 192–204.